BIOLOGY OF REPRODUCTION (2014) **90**(3):64, 1–11
Published online before print 29 January 2014.
DOI 10.1095/biolreprod.113.114645

Retinoic Acid Induces Multiple Hallmarks of the Prospermatogonia-to-Spermatogonia Transition in the Neonatal Mouse[1]

Jonathan T. Busada,[3] Evelyn P. Kaye,[3] Randall H. Renegar,[3] and Christopher B. Geyer[2,3,4]

[3]*Department of Anatomy and Cell Biology, Brody School of Medicine at East Carolina University, Greenville, North Carolina*
[4]*East Carolina Diabetes and Obesity Institute, Greenville, North Carolina*

ABSTRACT

In mammals, most neonatal male germ cells (prospermatogonia) are quiescent and located in the center of the testis cords. In response to an unknown signal, prospermatogonia transition into spermatogonia, reenter the cell cycle, divide, and move to the periphery of the testis cords. In mice, these events occur by 3–4 days postpartum (dpp), which temporally coincides with the onset of retinoic acid (RA) signaling in the neonatal testis. RA has a pivotal role in initiating germ cell entry into meiosis in both sexes, yet little is known about the mechanisms and about cellular changes downstream of RA signaling. We examined the role of RA in mediating the prospermatogonia-to-spermatogonia transition in vivo and found 24 h of precocious RA exposure-induced germ cell changes mimicking those that occur during the endogenous transition at 3–4 dpp. These changes included: 1) spermatogonia proliferation; 2) maturation of cellular organelles; and 3), expression of markers characteristic of differentiating spermatogonia. We found that germ cell exposure to RA did not lead to cellular loss from apoptosis but rather resulted in a delay of ~2 days in their entry into meiosis. Taken together, our results indicate that exogenous RA induces multiple hallmarks of the transition of prospermatogonia to spermatogonia prior to their entry into meiosis.

developmental biology, gamete biology, retinoids, spermatogonia, testis

INTRODUCTION

Following sex determination, primordial germ cells in male mice become prospermatogonia at ~12.5 days postcoitum (dpc), proliferate briefly, and become arrested in G0/G1 of the cell cycle from 14.5 dpc until 1–2 days postpartum (dpp) [1–4]. Then, in response to an undefined signal(s), they move from a central position to the periphery of the testis cords and resume mitosis as spermatogonia. Completion of both migration and mitosis is required for their continued survival [2]. This move positions them in a potential stem cell niche, flanked by Sertoli cells within the cord and peritubular myoid cells outside the cord. The transition of quiescent prospermatogonia into distinct proliferating populations of type A spermatogonia marks the beginning of spermatogenesis. One population of undifferentiated type A spermatogonia (A_s-A_{al}) retains stem cell potential to ensure long-term maintenance of the germline through balanced self-renewal and differentiation, whereas the other population of differentiating type A spermatogonia ($A_{1–4}$) is thought to be committed to ultimately enter meiosis (reviewed in references [5–7]). The first wave of spermatogenesis does not rely upon stem cell function but rather on differentiating spermatogonia that arise directly from the founding pool of prospermatogonia [8]. It has been suggested that germ cells that fail to make this transition provide the source for carcinoma in situ, the precursor lesion to most testicular germ cell tumors in humans [9–11].

RA has a central role in regulating the sex-specific timing of meiotic initiation in mouse germ cells [12–16]. RA is produced by the mesonephroi of both sexes by 13.5 dpc and enters the adjacent gonad. In the fetal ovary, RA signaling coincides with meiotic initiation at 13.5 dpc [12, 16], although there its role remains to be clarified [17]. In contrast, RA in the fetal testis is degraded by CYP26 enzymes such as CYP26B1, effectively blocking RA signaling in prospermatogonia [12, 16, 18]. Differentiation leading to meiotic initiation is therefore delayed until 3–4 dpp in the testis when RA is no longer actively degraded [12, 16, 19]. The current understanding of RA function in the neonatal testis in vivo is rather limited. The only currently known specific role of RA is activation of the germ cell-specific *Stra8* gene, which encodes a protein that is essential for germ cell development, although its precise role is unknown [20–22]. It was previously shown that neonatal RA injection led to transient increases in *Stra8* and *Sycp3* mRNA and protein levels after 24 h [23], followed by a modest increase in germ cell apoptosis [23, 24]. These neonatal RA injections resulted in significant stage synchronization in the adult [23, 24]. In other studies, spermatogonial differentiation was blocked in prepubertal mice in 2 genetic models with defective RA storage or production, respectively [25, 26]. Despite intense interest in the processes of germ cell differentiation and meiotic initiation, little is known about the cellular changes that occur downstream of RA during germ cell development.

In this study, we administered exogenous RA to mice at 1 dpp (2 days before their endogenous exposure) and determined the downstream consequences for germ cell development. We found precocious RA exposure-induced germ cell changes mimicking those that occur during the endogenous transition. These include: 1) proliferation, 2) maturation of cellular organelles, and 3) expression of markers characteristic of differentiating spermatogonia. We then followed the fate of these spermatogonia for several days and found that they were not lost by apoptosis but rather became transiently arrested before entering meiosis 2–3 days later than controls. This temporary arrest coincided with a transient increase in the expression of *Cyp26a1* and *Cyp2b1*, which encode RA-

[1]Supported by National Institutes of Health/National Institute of Child Health and Development grant HD072552 to C.B.G.
[2]Correspondence: Christopher B. Geyer, Brody School of Medicine at East Carolina University, Greenville, NC 27834.
E-mail: geyerc@ecu.edu

Received: 3 October 2013.
First decision: 5 November 2013.
Accepted: 24 January 2014.

eISSN: 1529-7268 http://www.biolreprod.org
ISSN: 0006-3363

degrading enzymes. This unexpected delay in meiotic entry following early RA exposure suggests that a consistent source of RA is required for neonatal germ cell progression to meiosis.

MATERIALS AND METHODS

Neonatal Mouse Injection and Tissue Fixation

All procedures using animals were performed according to the guidelines outlined in the National Research Council Guide for the Care and Use of Laboratory Animals and approved by the Animal Care and Use Committee at East Carolina University (AUP no. A178). CD-1 mice were used for all studies, and the day of birth was designated as 0 dpp. Neonatal mice received one subcutaneous injection of 50 or 100 μg of all-*trans*-RA (catalog no. R2625; Sigma-Aldrich) dissolved in dimethyl sulfoxide (DMSO) or DMSO alone at 1 dpp. Bromodeoxyuridine (BrdU; catalog no. B9285; Sigma-Aldrich) was dissolved in DMSO and 50 μg/g body weight was injected with or without RA. Mice were euthanized by decapitation at various time points after injections. Testes were then collected and either snap-frozen in liquid nitrogen and stored at −80°C or fixed in 4% paraformaldehyde (PFA) for cryosectioning or in Bouin solution (for histological analysis).

Quantitative RT-PCR

Quantitative RT-PCR (qRT-PCR) was performed with RNA isolated from whole testis lysates, using Trizol reagent (Life Technologies) according to the manufacturer's instructions and then quantitated by ultraviolet spectroscopy. Fifty nanograms of RNA were reverse-transcribed and subjected to qPCR in the same reaction tube using iScript One-Step RT-PCR kit with SYBR green (Bio-Rad). Amplification and detection of specific gene products were performed using an iCycler IQ (Bio-Rad) real-time PCR detection system. Threshold temperatures were selected automatically, and all amplifications were followed by melt-curve analysis. Relative mRNA levels were calculated using the delta-delta cycle threshold (ΔΔCt) method: mRNA fold-change level = $(2^{-\Delta\Delta Ct})$, where ΔΔCt = [ΔCt gene of interest in treated group] − [ΔCt of gene of interest in control group], where ΔCt = the [Ct gene of interest] – [Ct of reference gene]. Ct values were normalized to those of *Rpl19*, and qRT-PCR was performed in triplicate with testes from at least 4 animals.

Histology and Indirect Immunofluorescence

Whole testes fixed in Bouin solution for 2 h at 4°C were washed overnight in 1× PBS, dehydrated through an ethanol series, processed using standard methods, and then embedded in paraffin and cut into 5-μm sections. Sections were stained with hematoxylin and eosin (H&E) stain using standard methods. Immunohistochemistry (IHC) of Bouin-fixed sections using anti-RHOX13 was done as described previously [27, 28].

Indirect immunofluorescence (IIF) was performed using standard methods. Briefly, 5-μm frozen sections were cut from tissues that were fixed in 4% PFA and embedded in OCT. Blocking and antibody incubations were carried out in 1× PBS containing 3% BSA plus 0.1% Triton X-100, and stringency washes were done with 1× PBS plus 0.1% Triton X-100. For staining with anti-BrdU, sections were first incubated in 2M HCl for 1 h at 37°C to expose epitopes. All sections were blocked for 30 min at room temperature and then incubated in primary antibody for 1 h at room temperature or overnight at 4°C. Primary antibody was omitted as a negative control. Primary antibodies used were anti-ZBTB16/PLZF (1:500 dilution, no. 22839, Santa Cruz Biotechnology), anti-STRA8 (1:3000 no. 49–602, Abcam), anti-KIT (1:1000 dilution, no. 3074, Cell Signaling Technology), anti-SOHLH1 (1:1000 dilution, a gift from A. Rajkovic, U. of Pittsburgh [29]), activated anti-cleaved CASP3 (1:500 dilution, no. 9664, Cell Signaling Technology), anti-MKI67 (1:500 dilution, no. 15580, Abcam), anti-BrdU (1:50 dilution, no. 00–0103, Life Technologies), and anti-cleaved PARP1 (1:400 dilution, no. 9544, Cell Signaling Technology). Secondary antibody (1:500 dilution, Alexa Fluor-488 or −594 donkey anti-rabbit immunoglobulin G [IgG], Invitrogen) plus phalloidin-594 (1:500 dilution, Invitrogen) were applied for 1 h at room temperature. Coverslips were mounted with Vectastain containing 4′,6-diamidino-2-phenylindole (DAPI; Vector Laboratories), and images were obtained using a Fluoview FV1000 confocal laser scanning microscope (Olympus America). IIF and IHC were performed in triplicate with testes from at least 4 animals.

Cell Counting

Male germ cells were manually counted from IIF photomicrographs captured with an Axio Observer A1 microscope (Carl Zeiss Microscopy, LLC) equipped with an XL16C digital camera and Exponent version 1.3 software (Dage-MTI). Germ cells were stained by IIF using antibodies against ZBTB16/PLZF (see above), and testis cords were visualized by staining with phalloidin-594 (see above). Photomicrographs were analyzed using Axiovision software (Carl Zeiss Microscopy, LLC). Testis cords were outlined manually using phalloidin staining as a guide, and the total germ cell numbers were divided by total cord surface area and multiplied by 1000 to obtain cells/mm^2. Cell counting was performed in duplicate on testes from at least 4 animals.

Electron Microscopy

Testes were cut into 1- to 3-mm pieces and fixed for 2 h in 2% glutaraldehyde and then post-fixed in 1% osmium tetroxide (Stevens Metallurgical). Tissues were then dehydrated by passage through an ethanol series and embedded in Spurr medium (Electron Microscopy Sciences). Tissues were cut into ultrathin sections (70 nm) and placed on fresh plasma-etched 200-hexagon mesh copper grids (Electron Microscopy Science). Sections were stained in saturated uranyl-acetate in 50% ethanol for 30 min at room temperature in a humid chamber, washed in distilled water, and then stained with Reynold lead citrate for 5 min at room temperature. Sections were viewed with a 1200 EX electron microscope (JEOL) at 80-kV accelerating voltage. Images were recorded using an SIS MegaView III charge-coupled device camera (Olympus). Electron microscopy was performed using testes from 6 different animals.

Statistics

Statistical analyses were performed using the Student *t*-test. Statistical significance was set at a P value of ≤ 0.05.

RESULTS

Neonatal RA Treatments Induce Stra8 Expression

RA provides the requisite signal for the development of spermatogonia in juvenile and adult mice [14, 30–32]. To study the effects of RA on neonatal testis development, we adapted an in vivo model in which neonatal mice were injected with all-*trans*-RA at 1 dpp, 2 days prior to their normal endogenous exposure at 3–4 dpp (Fig. 1A) [19]. Expression of *Stra8* mRNA and protein provided evidence of RA signaling in germ cells, and both were detectable by 3–4 dpp in a subset of spermatogonia (Fig. 1, B and C) [19, 23]. This timing coincides with the natural prospermatogonia-to-spermatogonia transition in the neonatal mouse testis. Injection of 50 or 100 μg of exogenous RA at 1 dpp significantly increased the number of STRA8-positive germ cells (~18-fold), observed by IIF, relative to DMSO-treated controls (Fig. 1, D and E, and see Supplemental Fig. S1; supplemental data are available online at www.biolreprod.org), and induced *Stra8* mRNA similar to the levels measured in 4-dpp testes (Fig. 1F). Similar *Stra8* induction has been shown previously following RA injection into mice at 2 dpp [30]. Both of the doses of RA consistently induced STRA8 protein. However, injection of 100 μg of RA reduced animal survival rates after 48 h, so we used 50 μg for experiments that involved longer periods prior to euthanasia.

RA Stimulates Proliferation of Neonatal Germ Cells

The male germ cell population approximately doubles from 1 to 4 dpp in the mouse [33], and this reflects a reentry into the cell cycle as prospermatogonia transition to spermatogonia (reviewed in [34]). The timing of germ cell proliferation corresponds with onset of RA signaling in the neonatal testis [19, 30]. We therefore hypothesized that, prior to its proposed role in meiotic initiation (at 8–10 dpp in the mouse), RA directs postnatal expansion of the germ cell population. To test this hypothesis, we injected mice with DMSO or RA at 1 dpp, euthanized them 24 h later, and then stained germ cells with MKI67, an established marker of nuclear proliferation [35]. We detected a dramatic increase in the number of MKI67-positive

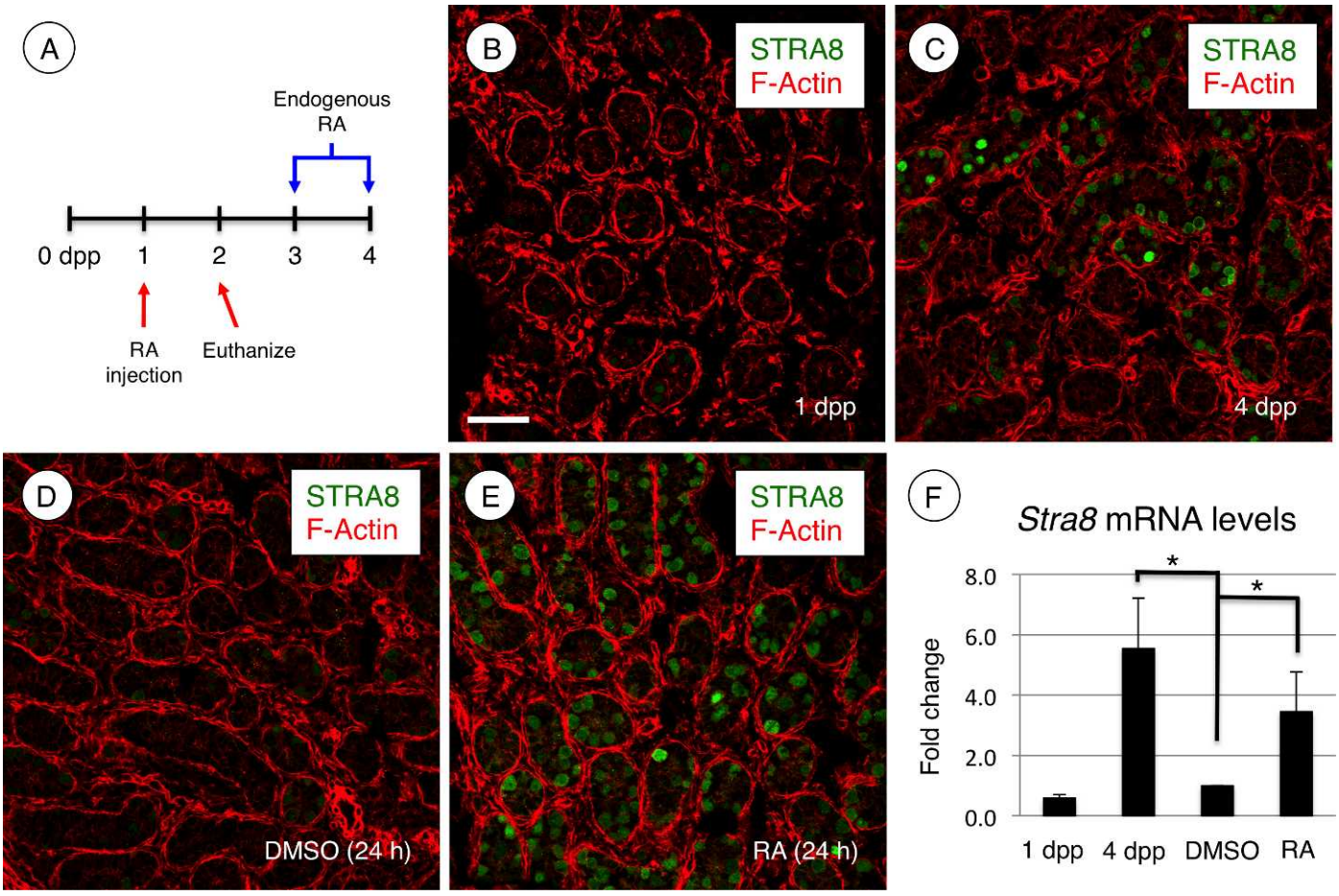

FIG. 1. RA treatment induced expression of *Stra8* mRNA and protein. **A**) Neonatal mice were injected at 1 dpp and euthanized 24 h after injection. The normal endogenous RA signaling is initiated at 3 to 4 dpp. **B**–**E**) IIF was performed to detect STRA8 (green), and cords were counterstained with phalloidin (red). Testes were from untreated mice aged 1 dpp (**B**) or 4 dpp (**C**) or were from mice euthanized 24 h after injection at 1 dpp with DMSO (**D**) or RA (**E**). **F**) *Stra8* mRNA levels were quantitated from 1- and 4-dpp testes as well as from testes from mice injected at 1 dpp with either DMSO or RA and euthanized 24 h later. Message levels were normalized to the DMSO-treated group, which was set at 1. Bar = 60 μm. *$P < 0.01$.

(MKI67+) germ cells (identified by appearance and diameter of DAPI-stained nuclei) in response to RA (Fig. 2, A and B). To verify that the MKI67+ cells that had reentered the cell cycle were indeed germ cells, we first injected mice at 1 dpp with BrdU and either DMSO or RA. We then harvested testes and performed co-IIF with anti-BrdU and anti-ZBTB16 and found that 25% ± 2.1% of ZBTB16+ cells in DMSO-treated testes were positive for BrdU. In contrast, 40% ± 9.7% of ZBTB16+ cells were also BrdU+, which was a significant increase ($P = 0.015$), and indicated that RA stimulated more germ cells to replicate their DNA in preparation for cell division (Supplemental Fig. S2).

We quantified the increased number of male germ cells in DMSO- and RA-treated mice. Discrimination between Sertoli and germ cell nuclei is rather straightforward in DAPI-stained sections of the neonatal testis; the small ovoid Sertoli cell nuclei contain intense heterochromatic foci, whereas both prospermatogonia and spermatogonia nuclei are large and round and contain very little heterochromatin [36]. We identified germ cells by using these criteria along with staining for DDX4, a pan-germ cell marker (Supplemental Fig. S3, [37, 38]). In addition, we labeled germ cells with anti-ZBTB16 (also called PLZF), which is expressed in prospermatogonia and spermatogonia [39, 40], and found that all germ cells in the neonatal testis were ZBTB16+ (Fig. 2, C and D). Therefore, we counted ZBTB16-positive germ cells in both treatment groups (Fig. 2, E and F) and expressed the totals as the fold-change in ZBTB16+ germ cells per square millimeter of testis cord (Fig. 2G). This approach accounted for the various sizes and shapes of cord sections and the seemingly stochastic number of total germ cells per cord. In testes from RA-treated mice, there were ~1.4-fold more ZBTB16+ germ cells than in vehicle controls (Fig. 2G). Quantitation of DDX4+ germ cells gave similar results (1.43-fold increase [Supplemental Fig. S3]).

RA Induces Expression of Differentiation Markers in Spermatogonia

The injection of exogenous RA induced precocious expression of *Stra8* and *Sycp3* mRNAs and STRA8 protein in neonatal male germ cells after 24 h (Fig. 1) [23]. To address whether RA induced expression of markers characteristic of differentiating spermatogonia, we stained DMSO- and RA-treated testes for SOHLH1 and KIT proteins (Fig. 3, A–D). KIT protein was detectable in some Leydig cells as previously reported [41, 42], and there was no increase in KIT+ interstitial cells in response to RA. There were a very small number of germ cells in which KIT was faintly detectable in DMSO-treated testes (Fig. 3A). However, treatment with exogenous RA at 1 dpp caused a dramatic increase in the number and staining intensity of KIT+ germ cells (Fig. 3B). Similarly,

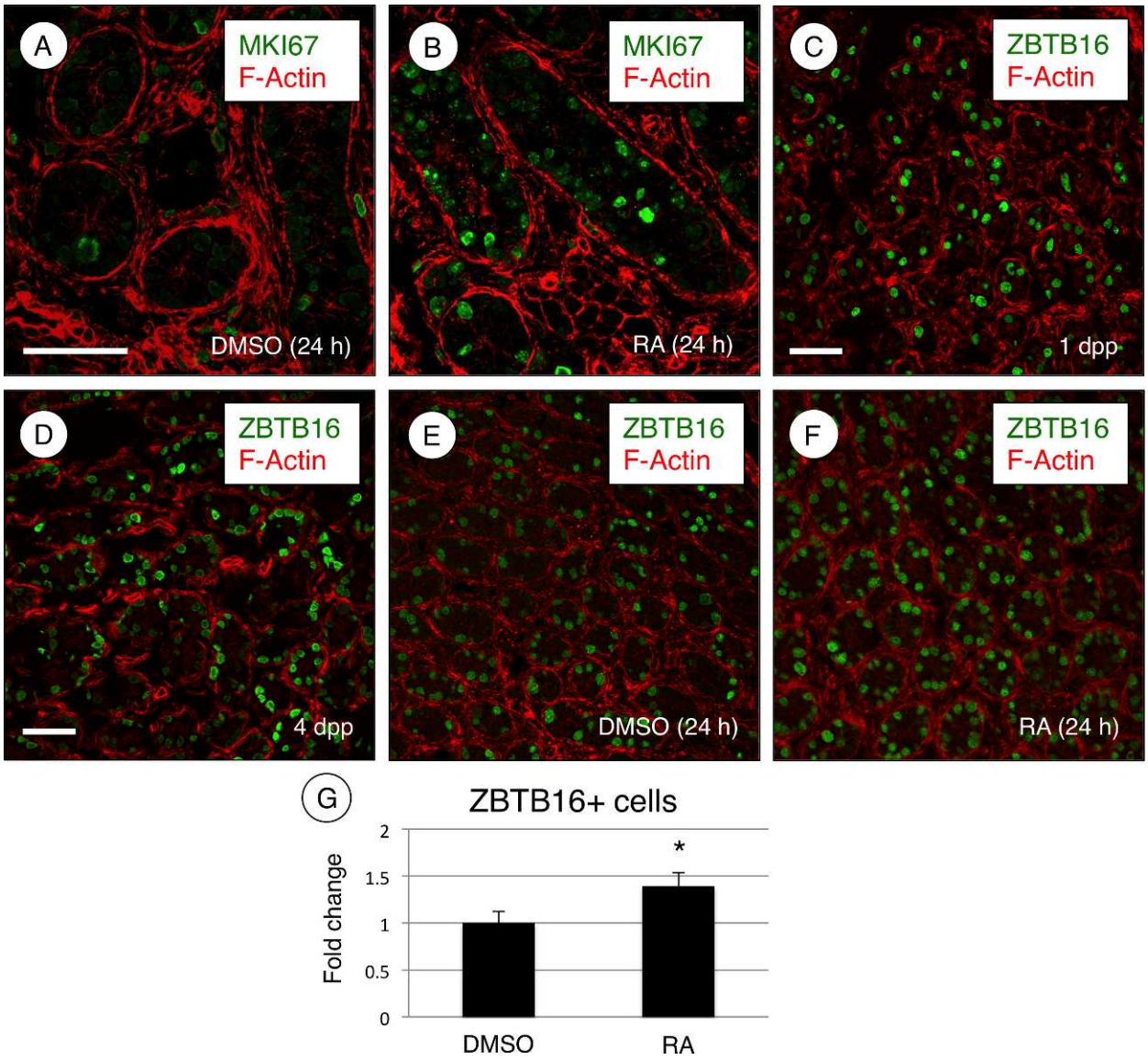

FIG. 2. RA treatment stimulated germ cell proliferation. IIF was performed with testis sections from mice injected with DMSO (**A** and **E**) or RA (**B** and **F**) at 1 dpp and euthanized 24 h later, and from mice aged 1 dpp (**C**) and 4 dpp (**D**). Five-micrometer sections were used for detection of MKI67 (**A** and **B**, both green) or ZBTB16 (**C**–**F**, both green), and phalloidin (red) was added to highlight the outline of the testis cords. **G**) The total numbers of ZBTB16+ cells were determined, divided by the total cord area and then multiplied by 1000 to get cells/mm^2, and reported as a fold change from the DMSO-treated group. Error bars are SD. Bars = 60 μm. *$P = 0.007$.

germ cells in DMSO-treated testes expressed low levels of SOHLH1 (Fig 3C), which increased dramatically following treatment with RA (Fig 3D).

RA Treatment Stimulates Germ Cell Mitochondria Biogenesis and Golgi Maturation

A number of studies painstakingly characterized changes in the ultrastructure of prospermatogonia and spermatogonia, including mitochondrial and Golgi morphologies [2, 43–45]. In agreement with these reports, we found that mitochondria in prospermatogonia at 1 dpp were relatively undeveloped and appeared round with few, indistinct cristae (Fig. 4, A–C). Few prospermatogonia had visible Golgi bodies, and those present consisted of 2–3 laminar stacks and few accompanying vesicles (Fig. 4, A–C). However, by 4 dpp, most germ cell mitochondria had increased numbers of cristae (Fig. 4, D–F) and Golgi complexes were more numerous, with extensive laminar stacks and large numbers of budding vesicles (Fig. 4, D–F). Treatment of mice with DMSO did not result in an appreciable change in mitochondria or Golgi complexes as compared to those at 1 dpp (Fig. 4, G–I). In stark contrast, RA treatment resulted in mitochondria with an increased number of electron-dense cristae, and Golgi bodies resembled those in 4-dpp germ cells (Fig. 4, J–L).

Precocious Exposure to RA Does Not Cause Neonatal Germ Cell Apoptosis

We tested whether 24-h exposure to RA following injection at 1 dpp induced germ cell apoptosis as was shown previously, following exposure of fetal and neonatal prospermatogonia to RA [23, 24, 46, 47]. We assessed germ cell apoptosis at 48 h (age = 3 dpp) and 72 h (age = 4 dpp) following RA administration by using 3 different methods: 1) IIF using antibodies to detect an active caspase (cleaved CASP3) and a

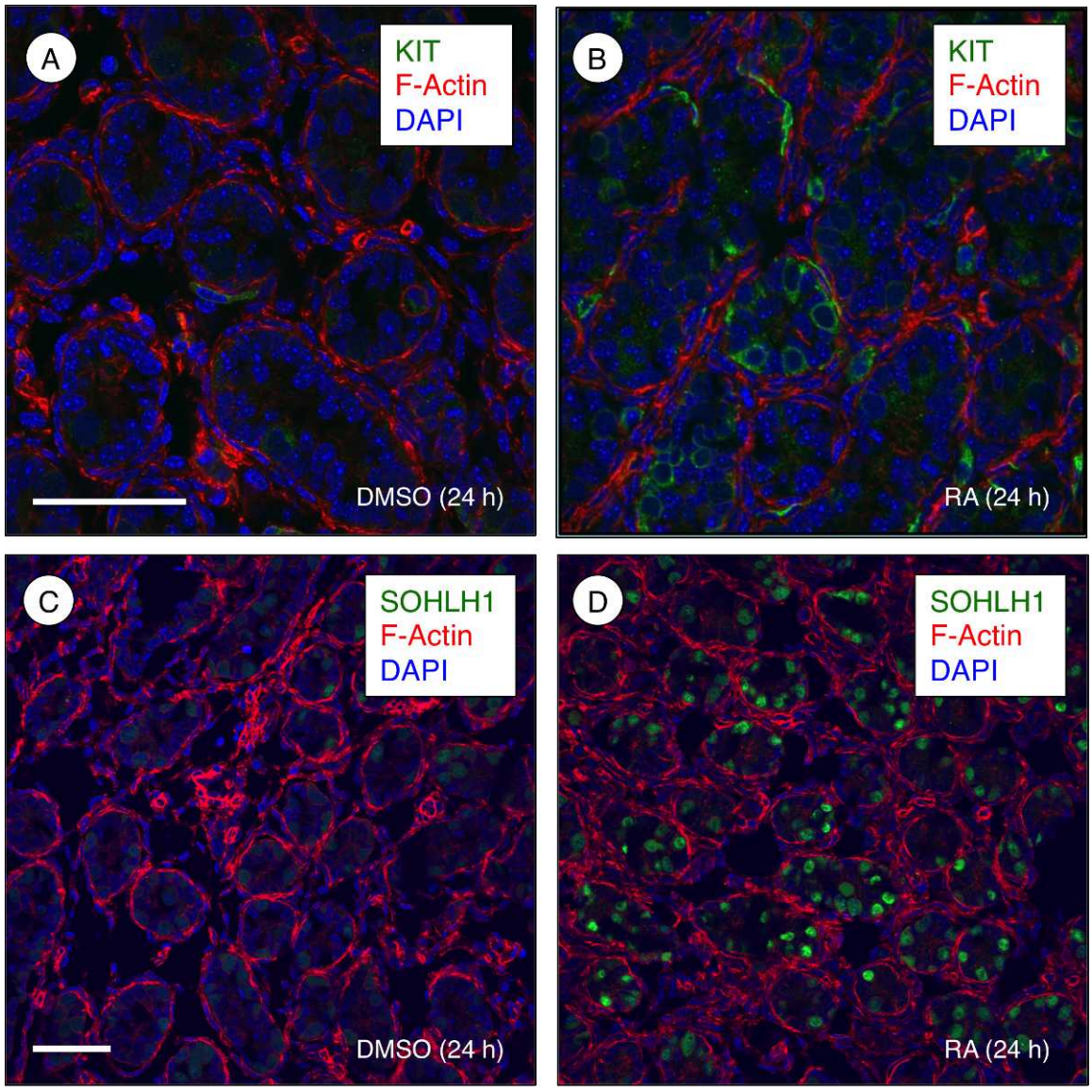

FIG. 3. RA treatment induced expression of the differentiation markers KIT and SOHLH1. IIF was performed with testis sections from mice euthanized 24 h after injection with DMSO (**A** and **C**) or RA (**B** and **D**) using antibodies for KIT (**A** and **B**, both green) or SOHLH1 (**C** and **D**, both green), and phalloidin (red) was added to visualize testis cords. Bar = 60 μm.

caspase cleavage target (PARP1); 2) quantitation of the germ cell population; and 3) histological analysis of H&E-stained sections to quantitate cells with apoptotic features. We found no significant increase in cleaved PARP1 in response to RA compared to that in DMSO controls at 48 or 72 h after injection (Fig. 5, A–E). Similar results were obtained by staining for cleaved CASP3 (Supplemental Fig. S4). Furthermore, there was no decrease in the germ cell population by 48 or 72 h post-RA treatment (Fig. 5F), as would be expected if there was an increase in cell death. Finally, light microscopy analysis revealed similar numbers of germ cells with apoptotic morphology in the RA- and DMSO-treated testes at 48 and 72 h after RA treatment (Supplemental Fig. S5). Results from a previous study indicated that RA injection at 2 dpp resulted in a modest increase in germ cell apoptosis after 48 h [23]. We repeated those experiments by injecting mice at 2 dpp and euthanizing them 48 h later, but we did not detect an increase in apoptosis as assessed by staining for cleaved CASP3 (Supplemental Fig. S6). Taken together, our results reveal that RA does not promote germ cell apoptosis when given during the prospermatogonia-to-spermatogonia transition.

Effects of RA on the Fate of Spermatogonia and Onset of Meiosis

Our results indicate that precocious RA exposure (at 1 dpp) caused prospermatogonia to exhibit characteristics of early differentiating spermatogonia (proliferation and marker gene expression) and then that these spermatogonia were not removed by apoptosis. An open question is whether the germ cell population in RA-injected mice follows a normal timeline to enter meiosis at 10 dpp or whether the timing of their entry into meiosis would be affected. To address this, we injected mice with either DMSO or 50 μg of RA at 1 dpp and then harvested testes at 6, 8, 10, 12, and 14 dpp to determine when the germ cell population entered meiosis. The reliable identification of specific premeiotic and meiotic germ cell types was made possible based on their location within the testis cord and characteristic nuclear diameter [36] and

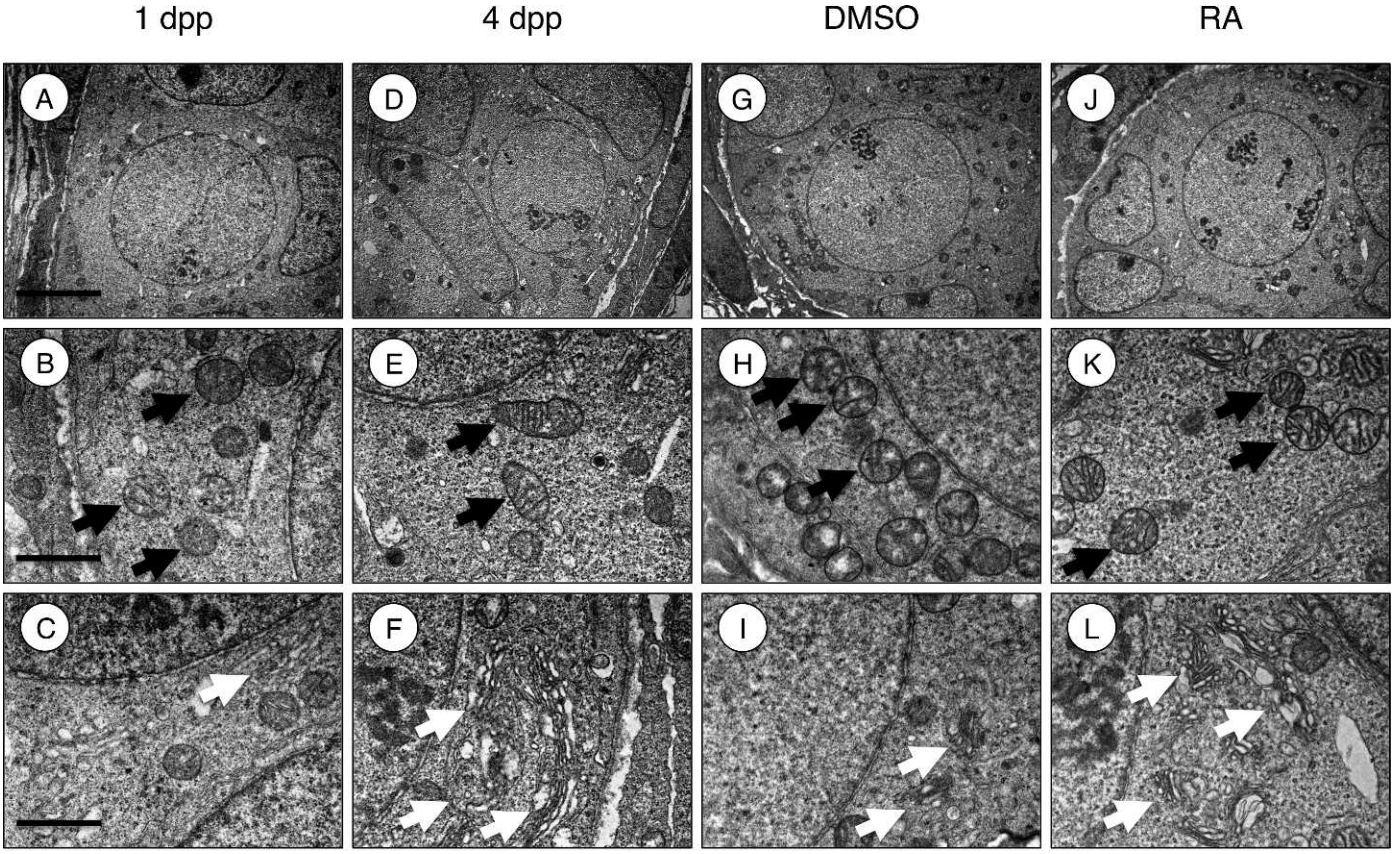

FIG. 4. RA treatment increased mitochondrial biogenesis and Golgi body development. Transmission electron micrographs show testes from mice aged 1 dpp (**A**–**C**) or 4 dpp (**D**–**F**) or those euthanized 24 h after treatment with DMSO (**G**–**I**) or RA (**J**–**L**). Black arrows indicate mitochondria, and white arrows indicate Golgi stacks. **A** and **B**) At 1 dpp, prospermatogonia mitochondria have few electron-dense cristae. **D** and **E**) Spermatogonia mitochondria from 4-dpp mice have numerous electron-dense cristae. **G** and **H**) Similarly, mitochondria in germ cells from DMSO-treated testes have few electron-dense cristae, whereas those of RA-treated testes (**J** and **K**) contain numerous electron-dense cristae. Golgi bodies in prospermatogonia from 1-dpp (**C**) and DMSO-treated (**I**) testes appear small and indistinct, whereas Golgi bodies in germ cells from 4-dpp (**F**) and RA-treated (**L**) testes are larger and appear active. Bar, top row = 5 μm; bottom 2 rows = 1 μm.

chromatin appearance [48]. To aid identification, we also labeled cells with an antibody against RHOX13, which is readily detectable in differentiating spermatogonia and preleptotene spermatocytes, faintly detectable in leptotene spermatocytes, and undetectable in zygotene and pachytene spermatocytes [27, 28]. Although we previously found that RA enhanced translation of *Rhox13* mRNAs in neonatal testes [28], we did not detect any difference in the cell types expressing RHOX13 in DMSO- or RA-treated testes after 8 dpp. In testes from CD-1 mice injected with DMSO, the first meiotic leptotene spermatocytes appeared as early as 8 dpp in a small subset (5%) of testis cords (data not shown). By 10 dpp, meiotic leptotene spermatocytes were readily detectable [36] and present in a high number (~40%) of the testis cords (Fig. 6A). Zygotene spermatocytes appeared in CD-1 mice in significant numbers at 12 dpp [36]. We found them in 37% of cords at 12 dpp (Fig. 6B), with this percentage increasing to 63% by 14 dpp (Fig. 6C). In RA-treated testes at 8 dpp, 1% of cords contained meiotic leptotene spermatocytes (data not shown), similar to DMSO-treated controls. By 10 dpp, only 15% of cords from RA-treated testes contained leptotene spermatocytes (Fig. 6D), which was a significant reduction compared to DMSO controls. This percentage increased to 27% by 12 dpp (Fig. 6E) and to 86% at 14 dpp (Fig. 5F). A small number of zygotene spermatocytes appeared in RA-treated testes by 10 dpp, and they were present in 10% and 12% of cords by 12 dpp and 14 dpp, respectively (Fig. 6, D–F). No histological evidence of increased germ cell apoptosis in the RA-treated testes was observed at any of these ages examined (data not shown). A comparison of the temporal appearance and abundance of specific germ cell types in these samples revealed that the 10- and 12-dpp RA-treated testes resembled those from vehicle-treated testis of 8- and 10-dpp mice, respectively. These results indicate that, contrary to our expectation that precocious RA would promote early meiotic initiation, it instead resulted in a 2–3 day delay, and testes appeared synchronized by 14 dpp.

Synchronization Follows Loss of RA Signaling after Exogenous RA Treatment

It was previously shown that testicular *Stra8* and *Sycp3* mRNA levels increased 24 h after RA injection but then surprisingly decreased by 48 and 72 h later [23]. This coincided with a transient increase in mRNA levels for *Cyp26a1* and *Cyp26b1*, which encode RA-degrading enzymes [23]. We verified those results using qRT-PCR to measure *Cyp26a1* and *Cyp26b1* mRNA levels from whole testis lysates of mice euthanized 24, 48, and 72 h following injection with DMSO or RA at 1 dpp. By 24 h after treatment with RA, *Cyp26a1* and *Cyp26b1* mRNA levels were significantly increased; but, by 48 and 72 h after injection, *Cyp26a1* levels had significantly decreased below that of control levels, whereas *Cyp26b1* levels only were significantly reduced at 48 h post-RA treatment and

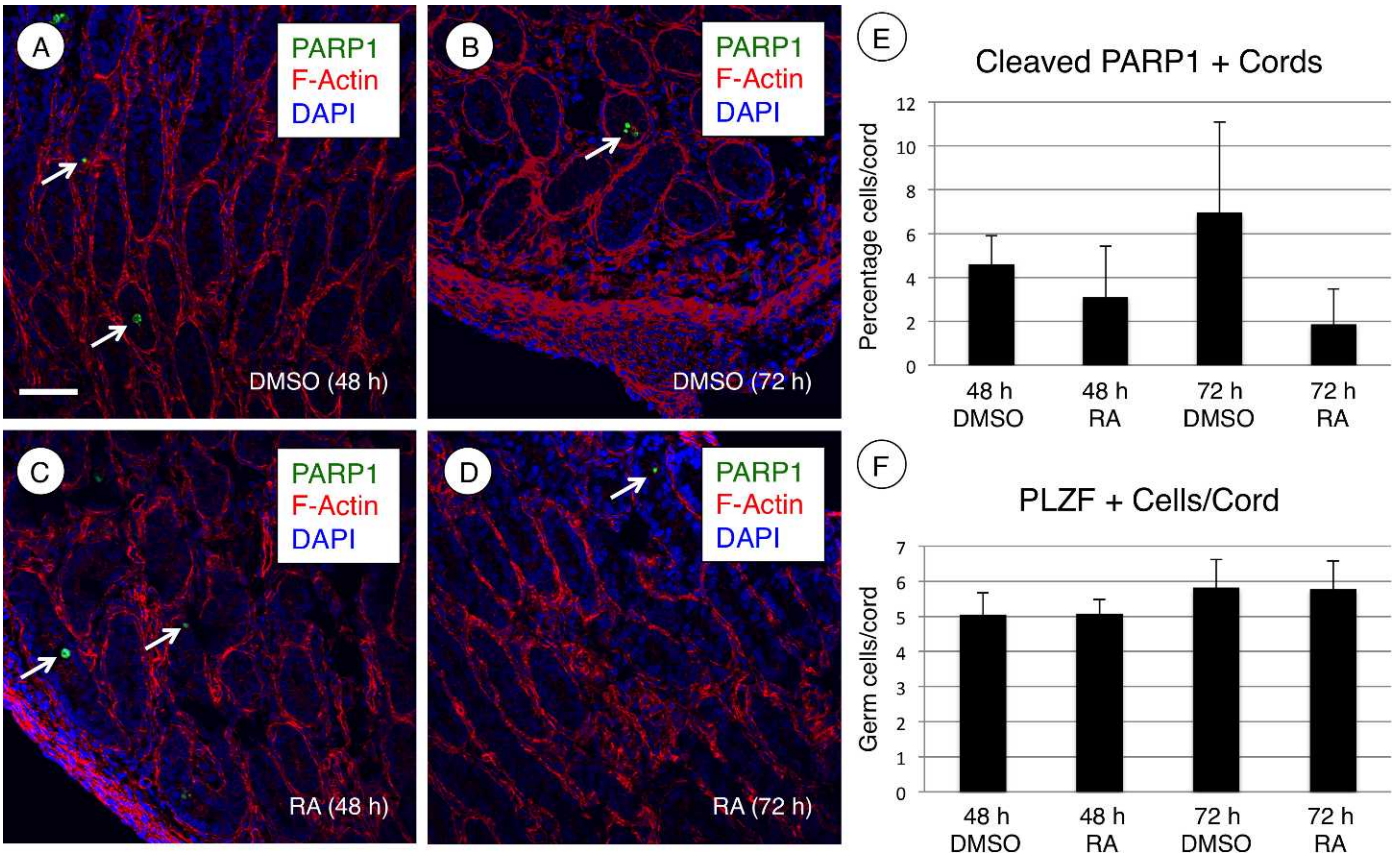

FIG. 5. Precocious RA exposure did not result in apoptosis. **A**–**D**) IIF of 5-μm sections from mice treated with DMSO (**A** and **B**) or RA (**C** and **D**) at 1 dpp and euthanized 48 h (**A** and **C**) or 72 h (**B** and **D**) later are shown. An antibody was used to detect cleaved PARP1 (green). Phalloidin was added to visualize the outlines of testis cords (red) and DAPI-labeled nuclei (blue). White arrows indicate cleaved PARP1+ cells. **E**) Testis cord cross-sections containing cells staining positive for cleaved PARP1 were counted, and their numbers were divided by total testis cord cross-sections and multiplied by 100 to obtain the percentage of cleaved PARP1+ cords. Error bars represent SD. **F**) The total number of ZBTB16+ cells were determined, divided by the total cord area, and then multiplied by 1000 to get cells/mm^2. This number was multiplied by the average area of a testis cross-section to determine the number of germ cells per testis cord cross-section. Error bars are SD. Bar = 60 μm.

returned to levels similar to those observed in DMSO-treated testes at 72 h post-RA treatment (Fig. 7, A and B). Furthermore, while *Stra8* mRNA and protein were dramatically increased 24 h after RA treatment (Fig. 1, E and F), by 48 and 72 h after RA treatment, *Stra8* mRNA levels were 10-fold and 7-fold decreased, respectively (Fig. 7C). Although STRA8 protein was readily detectable at 72 h post-DMSO, it became undetectable by 72 h after RA injection (Fig. 7D). *Stra8* mRNA levels increased from 48 to 72 h post-RA treatment, which follows the dramatic decrease in *Cyp26a1*. This suggests that endogenous testicular RA levels may be restored as CYP26 enzyme levels decrease.

DISCUSSION

The current study was designed to assess downstream events in neonatal germ cell development initiated by RA, which provides an essential trigger for meiotic entry in both sexes [12, 13, 16]. Currently, little is known about the molecular events initiated by RA signaling during the interval as prospermatogonia transition to spermatogonia. We exposed prospermatogonia to exogenous RA at 1 dpp at least 2 days earlier than their native exposure at 3–4 dpp. We discovered that early administration of RA induced precocious cellular proliferation and maturation of cellular organelles as well as expression of markers of differentiating spermatogonia. We then followed the fate of RA-exposed prospermatogonia and found that they were not subject to apoptosis but rather progressed to meiosis, although meiotic entry was delayed by ~2 days. This delay coincided with loss of RA signaling as assessed by loss of *Stra8* mRNA and protein. This indicates that, in contrast to fetal prospermatogonia, prospermatogonia in the neonatal testis have gained competence to differentiate in response to RA and do not undergo apoptosis.

When we injected exogenous RA into neonatal pups, there was increased proliferation, and a large percentage of spermatogonia became STRA8+ (Supplemental Fig. S1). In addition, RA-induced germ cell expression of both KIT and SOHLH1, which, along with STRA8, are established markers of differentiating spermatogonia. It was shown many years ago that dramatic ultrastructure changes occur as prospermatogonia make the transition to spermatogonia. In comparison with quiescent prospermatogonia, mitotically active spermatogonia have increased cytoplasm/nucleus ratios, mitochondria with increased numbers of cristae, and prominent Golgi complexes and rough endoplasmic reticulum [2, 43–45]. These features are commonly found in proliferating cells and are suggestive of increased energy metabolism to support biosynthetic activity. In particular, mitochondrial biogenesis increases the capacity for oxidative phosphorylation through expansion of the surface area of the inner mitochondrial membrane. A number of studies have documented the importance of mitochondrial biogenesis during differentiation of embryonic, hematopoietic, mesenchymal, and induced pluripotent stem cells. In general, undiffer-

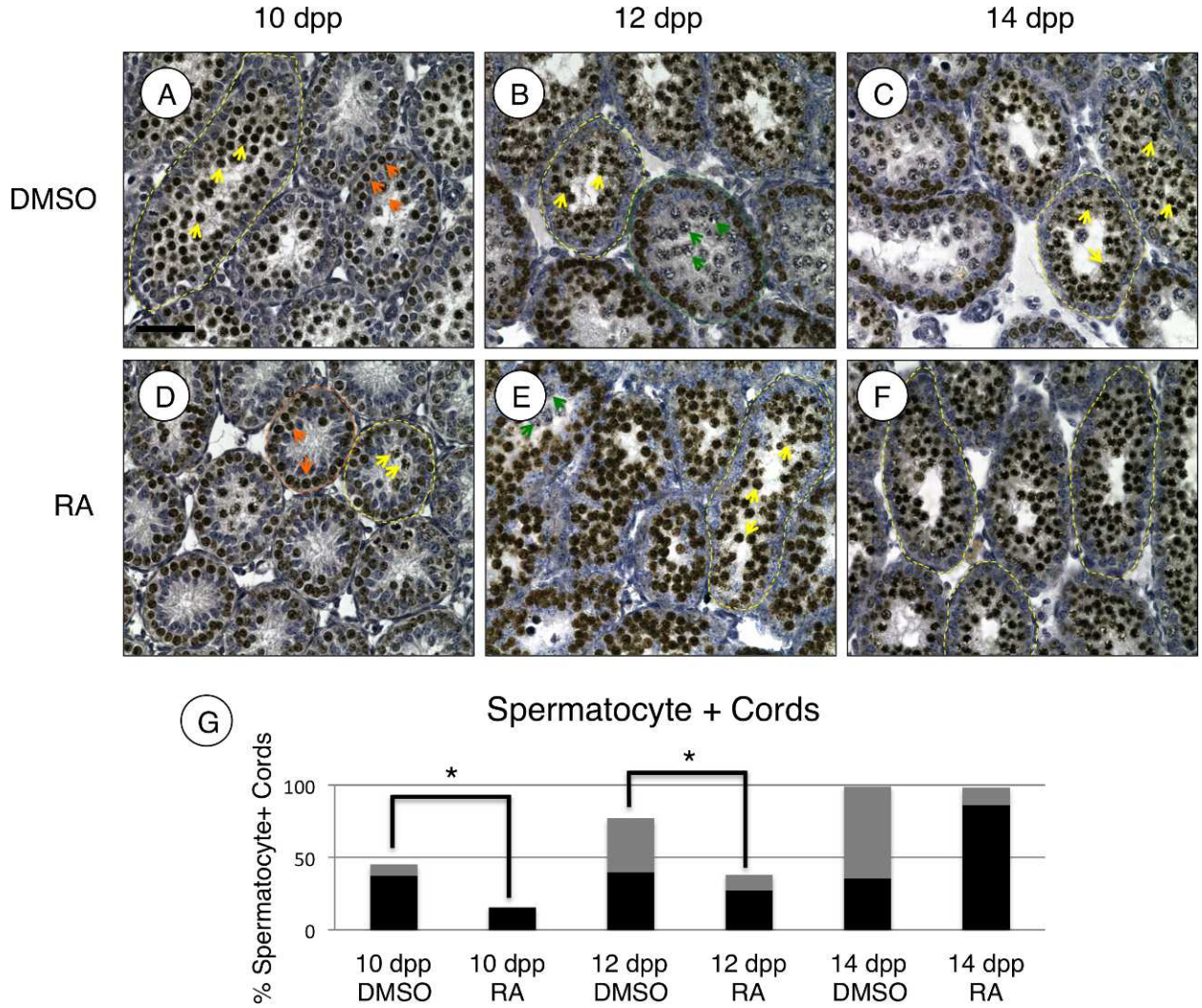

FIG. 6. Precocious RA exposure delayed meiotic entry. **A**–**F**) IHC was performed using testis sections from mice injected at 1 dpp with either DMSO (**A**–**C**) or RA (**D**–**F**). Ages of mice are shown at the top: 10 dpp (**A**, **D**), 12 dpp (**B**, **E**), and 14 dpp (**C**, **F**). An antibody was used to detect RHOX13 (brown), and sections were then counterstained with hematoxylin (blue). Orange arrows indicate preleptotene spermatocytes (**A**, **D**), yellow arrows indicate leptotene spermatocytes (**A**–**F**), and green arrows indicate zygotene spermatocytes (**B**, **C**, **E**). **G**) Leptotene and zygotene spermatocytes were quantitated in cord cross-sections from each age. The numbers of cords containing leptotene and zygotene spermatocytes were divided by the total number of cords analyzed, and the result was multiplied by 100 to obtain the percentage of cords containing meiotic leptotene/zygotene (meiotic) spermatocytes. Black bars represent leptotene-positive cords, and gray bars represent zygotene-positive cords. *$P < 0.01$ between total numbers of spermatocytes. Bar in **A** = 50 μm for **A**–**F**.

entiated stem cells tend to have reduced mitochondrial function and rely on glycolysis, whereas differentiating cells contain active mitochondria with high membrane potential and increased oxidative phosphorylation (reviewed in [49, 50]). The increased reactive oxygen species in differentiating cells as a result of oxidative metabolism are also linked to cellular differentiation [51, 52].

Fetal prospermatogonia exit the cell cycle at ~15.5 dpc and become quiescent until ~2–3 dpp in the mouse. This quiescent period is likely established because germ cells avoid exposure to RA by the expression of CYP26 enzymes such as CYP26B1 [12, 13, 16, 18], and this quiescence is arguably the least well-understood period of male germ cell development. It is clear that germ cells undergo paternal-specific DNA methylation patterning during this interval [53] and are sensitive to environmental insults that presumably generate heritable epigenetic lesions [54, 55]. When fetal prospermatogonia were exposed to RA, they expressed meiotic markers before dying by apoptosis [47, 56], indicating that they cannot commit to the meiotic program. In this study, we assessed whether postnatal prospermatogonia were similarly unable to both enter and proceed through meiosis. Administration of exogenous RA at 1 dpp (2–3 days prior to endogenous exposure) caused prospermatogonia to both enter and proceed through meiosis, albeit delayed, without dying by apoptosis. These results indicate that, unlike fetal prospermatogonia, neonatal spermatogonia prior to 4 dpp are competent to differentiate toward entering meiosis but are awaiting the RA signal to do so.

We found rather low numbers of apoptotic cells within testis cords of the neonatal testis. Regardless of DMSO or RA treatment, only ~5%–10% of cords contained cells expressing markers of apoptosis (cleaved CASP3 or PARP1) or had morphology consistent with apoptosis. These results are consistent with those from a previous study, where ~5% of testis cords in outbred ICR mice contained apoptotic cells from 3–7 dpp [57]. It was recently reported that apoptosis affected ~0.5 and 1 germ cell per testis cord in mice exposed at 2 dpp for 24 h with DMSO or RA, respectively [23]. These germ

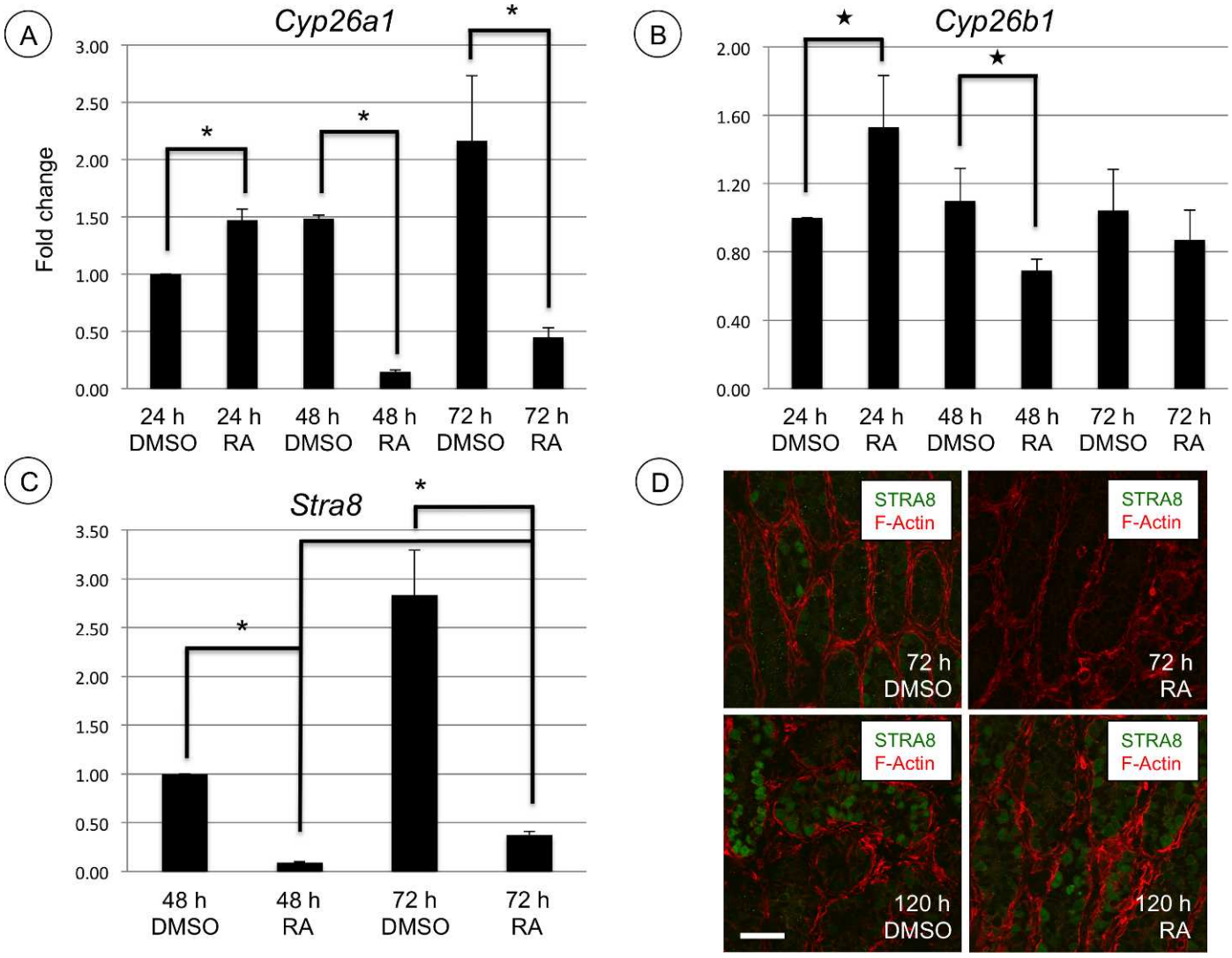

FIG. 7. RA treatment induced expression of RA-degrading enzymes. *Cyp26a1* (**A**), *Cyp26b1* (**B**), and *Stra8* (**C**) mRNAs were quantitated by qRT-PCR from mice euthanized 24, 48, and 72 h following treatment with DMSO or RA. **D**) IIF was performed to detect STRA8 (green), and F-actin was labeled with phalloidin (red) in testes harvested from mice 72 and 120 h after injection with either DMSO or RA. Error bars represent SD. *$P < 0.01$, stars $P < 0.05$. Bar = 40 μm.

cells stained positive for the activated effector caspase 3 but curiously did not display fragmented or condensed nuclei, shrunken cytoplasm, or detachment from the basement membrane, which are typical markers of apoptosis (reviewed in [58]). If the cleaved CASP3+ germ cells observed in that study were evenly distributed throughout the testis, it would mean that ~50% and ~100% of cords from DMSO- and RA-treated mice contained an apoptotic cell(s) respectively. However, based on our estimates that there are ~5 germ cells per testis cord at 3 dpp, an increase of 0.5 to 1 germ cell/cord in apoptosis in response to RA equals a 10% increase in apoptosis affecting the germ cell population. The neonatal male germ cells in the C57Bl/6 × 129 pups used in their studies were perhaps more susceptible to apoptosis than those in the CD-1 pups that we used. Even so, it is unlikely that such a modest increase in apoptosis (~10%) would result in the extensive stage synchronization seen both in that study and in the current one (in which apoptosis was not increased in response to RA).

The onset of RA signaling clearly has different consequences for the fate of male and female germ cells during development. Although RA signaling temporally coincides with meiotic entry of oocytes at ~13.5 dpc [16, 20, 59, 60], the onset of RA signaling in the testis occurs at 3–4 dpp [19, 30]. This creates a 5- to 7-day window between exposure of prospermatogonia to RA and appearance of the first meiotic leptotene spermatocytes by 8–10 dpp [36]. It is unclear why there is such a marked sex-specific difference in the initial response of germ cells to RA. However, female mammalian germ cells lack two important features found in the male: an analogous stem cell population and initial developmental asynchrony. The delay of approximately 1 wk between RA signaling and meiotic initiation corresponds to the time when the establishment of the spermatogonial stem cell population occurs in the neonatal testis [6]. By 4 dpp, only subsets of spermatogonia were STRA8+, which indicates that RA signaling does not occur in a significant proportion of spermatogonia at any particular time (in this study as well as in [19, 22, 30]). The expression of STRA8 in a limited number of germ cells indicates that there is a heterogeneous population of undifferentiated and differentiating spermatogonia by 3–4 dpp. The undifferentiated pool of spermatogonia appears to be protected from RA exposure (and remain STRA8-), whereas

RA signaling occurs in differentiating spermatogonia over the next 5–7 days.

Precocious neonatal exposure to RA accelerated germ cell development by approximately 48 h but then paradoxically delayed meiotic initiation by approximately 48 h 1 wk later. This was a rather surprising result, as we reasoned that if the timing between normal RA exposure (3–4 dpp) and meiotic initiation (8–10 dpp) were maintained, then meiosis would initiate 2 days early. Our results instead support a model whereby neonatal spermatogonia require multiple or consistent exposures to RA for committed differentiation to ultimately enter meiosis.

In agreement with previous studies done both in vitro and in vivo [23, 61], we detected increased testicular mRNA levels for the RA-degrading enzymes *Cyp26a1* and *Cyp26b1* after 24 h of exposure of 2-dpp mice to exogenous RA. In both this and previous studies, dramatic decreases in both *Cyp26a1* and *Cyp26b1* mRNA abundance were then seen after the initial increase following RA exposure [23, 61]. The CYP26 enzymes function to degrade RA, and their action has been implicated in protection of undifferentiated spermatogonia from inappropriate exposure to RA [12, 13, 16, 18, 30]. In this experimental paradigm, it is likely that an initial increase in CYP26A1 or CYP26B1 degrades not only the injected exogenous RA but also the endogenous RA. This is supported by our result indicating STRA8 is lost 48 h after RA injection (Fig. 7D). A loss of RA provides a plausible explanation for the stalled germ cell development resulting in the 2- to 3-day delay in meiotic initiation observed in our study. This model presumes that RA levels recover a few days after the decreased CYP26 enzyme levels, which then allows germ cells to proceed toward meiosis at the same pace. This is supported by our observation that *Stra8* mRNA levels significantly increase from 48 to 72 h following RA treatment (Fig. 7C). Such a model would explain the synchronization seen at 12 and 14 dpp in the current study and in adult mice in previous studies following modification of RA signaling [23, 24, 62]. It also reveals the fact that the initial differentiation of spermatogonia in response to RA (as indicated by their expression of STRA8, KIT, and SOHLH1) is reversible, as germ cells lose STRA8 expression after the increase in *Cyp26* levels but then can apparently differentiate 2 days later to enter meiosis.

The results of the current study indicate that RA provides an instructive signal for neonatal prospermatogonia to transition into spermatogonia. Hallmarks of differentiation such as germ cell proliferation, cord organization, and expression of differentiated spermatogonia markers, characteristic of spermatogonia were all observed approximately 2 days before their natural progression. In contrast to previous results, we found that neonatal exposure to RA does not increase germ cell apoptosis but causes precocious spermatogonia development that is then halted for ~2 days, presumably by increased CYP26-dependent degradation of RA. Once *Cyp26* levels decrease 48 h after RA exposure, endogenous RA levels are presumably restored, and differentiation continues such that synchrony of spermatogenesis is increased through adulthood.

ACKNOWLEDGMENT

The authors thank Joani Zary-Oswald for technical assistance, Dr. Aleksandar Rajkovich (University of Pittsburgh) for kindly providing the SOHLH1 antibody, and Dr. Brett Keiper (East Carolina University) for critically reading the manuscript.

REFERENCES

1. McCarrey JR. Toward a more precise and informative nomenclature describing fetal and neonatal male germ cells in rodents. Biol Reprod 2013; 89:47.
2. Roosen-Runge EC, Leik J. Gonocyte degeneration in the postnatal male rat. Am J Anat 1968; 122:275–299.
3. Vergouwen RP, Jacobs SG, Huiskamp R, Davids JA, de Rooij DG. Proliferative activity of gonocytes, Sertoli cells and interstitial cells during testicular development in mice. J Reprod Fertil 1991; 93:233–243.
4. Western P, Miles D, van den Bergen J, Burton M, Sinclair A. Dynamic regulation of mitotic arrest in fetal male germ cells. Stem Cells 2008; 26: 339–347.
5. de Rooij DG, Russell LD. All you wanted to know about spermatogonia but were afraid to ask. J Androl 2000; 21:776–798.
6. Oatley JM, Brinster RL. The germline stem cell niche unit in mammalian testes. Physiol Rev 2012; 92:577–595.
7. Yoshida S. Elucidating the identity and behavior of spermatogenic stem cells in the mouse testis. Reproduction 2012; 144:293–302.
8. Yoshida S, Sukeno M, Nakagawa T, Ohbo K, Nagamatsu G, Suda T, Nabeshima Y. The first round of mouse spermatogenesis is a distinctive program that lacks the self-renewing spermatogonia stage. Development 2006; 133:1495–1505.
9. Almstrup K, Ottesen AM, Sonne SB, Hoei-Hansen CE, Leffers H. Rajpert-De Meyts E, Skakkebaek NE. Genomic and gene expression signature of the pre-invasive testicular carcinoma in situ. Cell Tissue Res 2005; 322:159–165.
10. Kristensen DM, Sonne SB, Ottesen AM, Perrett RM, Nielsen JE, Almstrup K, Skakkebaek NE, Leffers H. Rajpert-De Meyts E. Origin of pluripotent germ cell tumours: the role of microenvironment during embryonic development. Mol Cell Endocrinol 2008; 288:111–118.
11. Sonne SB, Kristensen DM, Novotny GW, Olesen IA, Nielsen JE, Skakkebaek NE, Rajpert-De Meyts E, Leffers H. Testicular dysgenesis syndrome and the origin of carcinoma in situ testis. Int J Androl 2008; 31: 275–287.
12. Bowles J, Knight D, Smith C, Wilhelm D, Richman J, Mamiya S, Yashiro K, Chawengsaksophak K, Wilson MJ, Rossant J, Hamada H, Koopman P. Retinoid signaling determines germ cell fate in mice. Science 2006; 312: 596–600.
13. Bowles J, Koopman P. Retinoic acid, meiosis and germ cell fate in mammals. Development 2007; 134:3401–3411.
14. Gaemers IC, Sonneveld E, van Pelt AM, Schrans BH, Themmen AP, van der Saag PT, de Rooij DG. The effect of 9-cis-retinoic acid on proliferation and differentiation of a spermatogonia and retinoid receptor gene expression in the vitamin A-deficient mouse testis. Endocrinology 1998; 139:4269–4276.
15. Koshimizu U, Watanabe M, Nakatsuji N. Retinoic acid is a potent growth activator of mouse primordial germ cells in vitro. Dev Biol 1995; 168: 683–685.
16. Koubova J, Menke DB, Zhou Q, Capel B, Griswold MD, Page DC. Retinoic acid regulates sex-specific timing of meiotic initiation in mice. Proc Natl Acad Sci U S A 2006; 103:2474–2479.
17. Kumar S, Chatzi C, Brade T, Cunningham TJ, Zhao X, Duester G. Sex-specific timing of meiotic initiation is regulated by Cyp26b1 independent of retinoic acid signalling. Nat Commun 2011; 2:151.
18. MacLean G, Li H, Metzger D, Chambon P, Petkovich M. Apoptotic extinction of germ cells in testes of Cyp26b1 knockout mice. Endocrinology 2007; 148:4560–4567.
19. Zhou Q, Nie R, Li Y, Friel P, Mitchell D, Hess RA, Small C, Griswold MD. Expression of stimulated by retinoic acid gene 8 (Stra8) in spermatogenic cells induced by retinoic acid: an in vivo study in vitamin A-sufficient postnatal murine testes. Biol Reprod 2008; 79:35–42.
20. Anderson EL, Baltus AE, Roepers-Gajadien HL, Hassold TJ, de Rooij DG, van Pelt AM, Page DC. Stra8 and its inducer, retinoic acid, regulate meiotic initiation in both spermatogenesis and oogenesis in mice. Proc Natl Acad Sci U S A 2008; 105:14976–14980.
21. Mark M, Jacobs H, Oulad-Abdelghani M, Dennefeld C, Feret B, Vernet N, Codreanu CA, Chambon P, Ghyselinck NB. STRA8-deficient spermatocytes initiate, but fail to complete, meiosis and undergo premature chromosome condensation. J Cell Sci 2008; 121:3233–3242.
22. Oulad-Abdelghani M, Bouillet P, Decimo D, Gansmuller A, Heyberger S, Dolle P, Bronner S, Lutz Y, Chambon P. Characterization of a premeiotic germ cell-specific cytoplasmic protein encoded by Stra8, a novel retinoic acid-responsive gene. J Cell Biol 1996; 135:469–477.
23. Snyder EM, Davis JC, Zhou Q, Evanoff R, Griswold MD. Exposure to retinoic acid in the neonatal but not adult mouse results in synchronous spermatogenesis. Biol Reprod 2011; 84:886–893.
24. Davis JC, Snyder EM, Hogarth CA, Small C, Griswold MD. Induction of spermatogenic synchrony by retinoic acid in neonatal mice. Spermatogenesis 2013; 3:e23180.

25. Li H, Palczewski K, Baehr W, Clagett-Dame M. Vitamin A deficiency results in meiotic failure and accumulation of undifferentiated spermatogonia in prepubertal mouse testis. Biol Reprod 2011; 84:336–341.
26. Tong MH, Yang QE, Davis JC, Griswold MD. Retinol dehydrogenase 10 is indispensable for spermatogenesis in juvenile males. Proc Natl Acad Sci U S A 2013; 110:543–548.
27. Geyer CB, Eddy EM. Identification and characterization of Rhox13, a novel X-linked mouse homeobox gene. Gene 2008; 423:194–200.
28. Geyer CB, Saba R, Kato Y, Anderson AJ, Chappell VK, Saga Y, Eddy EM. Rhox13 is translated in premeiotic germ cells in male and female mice and is regulated by NANOS2 in the male. Biol Reprod 2012; 86:127.
29. Pangas SA, Choi Y, Ballow DJ, Zhao Y, Westphal H, Matzuk MM, Rajkovic A. Oogenesis requires germ cell-specific transcriptional regulators Sohlh1 and Lhx8. Proc Natl Acad Sci U S A 2006; 103: 8090–8095.
30. Snyder EM, Small C, Griswold MD. Retinoic acid availability drives the asynchronous initiation of spermatogonial differentiation in the mouse. Biol Reprod 2010; 83:783–790.
31. van Pelt AM, de Rooij DG. Retinoic acid is able to reinitiate spermatogenesis in vitamin A-deficient rats and high replicate doses support the full development of spermatogenic cells. Endocrinology 1991; 128:697–704.
32. van Pelt AM, van Dissel-Emiliani FM, Gaemers IC, van der Burg MJ, Tanke HJ, de Rooij DG. Characteristics of A spermatogonia and preleptotene spermatocytes in the vitamin A-deficient rat testis. Biol Reprod 1995; 53:570–578.
33. Chappell VA, Busada JT, Keiper BD, Geyer CB. Translational activation of developmental messenger RNAs during neonatal mouse testis development. Biol Reprod 2013; 89:61.
34. Culty M. Gonocytes, the forgotten cells of the germ cell lineage. Birth Defects Res C Embryo Today 2009; 87:1–26.
35. Scholzen T, Gerdes J. The Ki-67 protein: from the known and the unknown. J Cell Physiol 2000; 182:311–322.
36. Bellve AR, Cavicchia JC, Millette CF, O'Brien DA, Bhatnagar YM, Dym M. Spermatogenic cells of the prepubertal mouse. Isolation and morphological characterization. J Cell Biol 1977; 74:68–85.
37. Fujiwara Y, Komiya T, Kawabata H, Sato M, Fujimoto H, Furusawa M, Noce T. Isolation of a DEAD-family protein gene that encodes a murine homolog of *Drosophila* vasa and its specific expression in germ cell lineage. Proc Natl Acad Sci U S A 1994; 91:12258–12262.
38. Tanaka SS, Toyooka Y, Akasu R, Katoh-Fukui Y, Nakahara Y, Suzuki R, Yokoyama M, Noce T. The mouse homolog of *Drosophila* Vasa is required for the development of male germ cells. Genes Dev 2000; 14: 841–853.
39. Buaas FW, Kirsh AL, Sharma M, McLean DJ, Morris JL, Griswold MD, de Rooij DG, Braun RE. Plzf is required in adult male germ cells for stem cell self-renewal. Nat Genet 2004; 36:647–652.
40. Costoya JA, Hobbs RM, Barna M, Cattoretti G, Manova K, Sukhwani M, Orwig KE, Wolgemuth DJ, Pandolfi PP. Essential role of Plzf in maintenance of spermatogonial stem cells. Nat Genet 2004; 36:653–659.
41. Prabhu SM, Meistrich ML, McLaughlin EA, Roman SD, Warne S, Mendis S, Itman C, Loveland KL. Expression of c-Kit receptor mRNA and protein in the developing, adult and irradiated rodent testis. Reproduction 2006; 131:489–499.
42. Rothschild G, Sottas CM, Kissel H, Agosti V, Manova K, Hardy MP, Besmer P. A role for kit receptor signaling in Leydig cell steroidogenesis. Biol Reprod 2003; 69:925–932.
43. Baillie AH. The histochemistry and ultrastructure of the genocyte. Anat J 1964; 98:641–645.
44. Franchi LL, Mandl AM. The ultrastructure of germ cells in foetal and neonatal male rats. J Embryol Exp Morphol 1964; 12:289–308.
45. Gondos B, Renston RH, Conner LA. Ultrastructure of germ cells and Sertoli cells in the postnatal rabbit testis. Am J Anat 1973; 136:427–439.
46. Li H, Clagett-Dame M. Vitamin A deficiency blocks the initiation of meiosis of germ cells in the developing rat ovary in vivo. Biol Reprod 2009; 81:996–1001.
47. Trautmann E, Guerquin MJ, Duquenne C, Lahaye JB, Habert R, Livera G. Retinoic acid prevents germ cell mitotic arrest in mouse fetal testes. Cell Cycle 2008; 7:656–664.
48. Drumond AL, Meistrich ML, Chiarini-Garcia H. Spermatogonial morphology and kinetics during testis development in mice: a high-resolution light microscopy approach. Reproduction 2011; 142:145–155.
49. Chen CT, Hsu SH, Wei YH. Mitochondrial bioenergetic function and metabolic plasticity in stem cell differentiation and cellular reprogramming. Biochim Biophys Acta 2012; 1820:571–576.
50. Rehman J. Empowering self-renewal and differentiation: the role of mitochondria in stem cells. J Mol Med (Berl) 2010; 88:981–986.
51. Crespo FL, Sobrado VR, Gomez L, Cervera AM, McCreath KJ. Mitochondrial reactive oxygen species mediate cardiomyocyte formation from embryonic stem cells in high glucose. Stem Cells 2010; 28: 1132–1142.
52. Ito K, Hirao A, Arai F, Takubo K, Matsuoka S, Miyamoto K, Ohmura M, Naka K, Hosokawa K, Ikeda Y, Suda T. Reactive oxygen species act through p38 MAPK to limit the lifespan of hematopoietic stem cells. Nat Med 2006; 12:446–451.
53. Reik W, Dean W, Walter J. Epigenetic reprogramming in mammalian development. Science 2001; 293:1089–1093.
54. Anway MD, Cupp AS, Uzumcu M, Skinner MK. Epigenetic transgenerational actions of endocrine disruptors and male fertility. Science 2005; 308:1466–1469.
55. Daxinger L, Whitelaw E. Understanding transgenerational epigenetic inheritance via the gametes in mammals. Nat Rev Genet 2012; 13: 153–162.
56. Li H, MacLean G, Cameron D, Clagett-Dame M, Petkovich M. Cyp26b1 expression in murine Sertoli cells is required to maintain male germ cells in an undifferentiated state during embryogenesis. PLoS One 2009; 4: e7501.
57. Mori C, Nakamura N, Dix DJ, Fujioka M, Nakagawa S, Shiota K, Eddy EM. Morphological analysis of germ cell apoptosis during postnatal testis development in normal and Hsp 70-2 knockout mice. Dev Dyn 1997; 208: 125–136.
58. Taylor RC, Cullen SP, Martin SJ. Apoptosis: controlled demolition at the cellular level. Nat Rev Mol Cell Biol 2008; 9:231–241.
59. Baltus AE, Menke DB, Hu YC, Goodheart ML, Carpenter AE, de Rooij DG, Page DC. In germ cells of mouse embryonic ovaries, the decision to enter meiosis precedes premeiotic DNA replication. Nat Genet 2006; 38: 1430–1434.
60. Spiller CM, Bowles J, Koopman P. Regulation of germ cell meiosis in the fetal ovary. Int J Dev Biol 2012; 56:779–787.
61. Zhou Q, Li Y, Nie R, Friel P, Mitchell D, Evanoff RM, Pouchnik D, Banasik B, McCarrey JR, Small C, Griswold MD. Expression of stimulated by retinoic acid gene 8 (Stra8) and maturation of murine gonocytes and spermatogonia induced by retinoic acid in vitro. Biol Reprod 2008; 78:537–545.
62. Hogarth CA, Griswold MD. Retinoic acid regulation of male meiosis. Curr Opin Endocrinol Diabetes Obes 2013; 20:217–223.